Porous Materials

DOI: 10.1002/anie.201309836

Templated Synthesis of Nitrogen-Enriched Nanoporous Carbon Materials from Porogenic Organic Precursors Prepared by ATRP**

Dingcai Wu, Zhenghui Li, Mingjiang Zhong, Tomasz Kowalewski,* and Krzysztof Matyjaszewski**

Abstract: *A facile templated synthesis of functional nanocarbon materials with well-defined spherical mesopores is developed using all-organic porogenic precursors comprised of hairy nanoparticles with nitrogen-rich polyacrylonitrile shells grafted from sacrificial cross-linked poly(methyl methacrylate) cores (xPMMA-g-PAN). Such shape-persistent all-organic nanostructured precursors, prepared using atom transfer radical polymerization (ATRP), assure robust formation of template nanostructures with continuous PAN precursor matrix over wide range of compositions, and allow for removal of the sacrificial template through simple thermal decomposition. Carbon materials prepared using this method combine nitrogen enrichment with hierarchical nanostructure comprised of microporous carbon matrix interspersed with mesopores originating from sacrificial xPMMA cores, and thus perform well as CO_2 adsorbents and as supercapacitor electrodes.*

In modern materials science, there is considerable interest in the design and fabrication of nanoporous carbon materials with well-defined porosity, high surface area, good electrical conductivity, tunable surface chemistry, and high chemical and physical stability.[1] With such attributes, carbon materials of this kind are currently finding wide applications in many fields including energy, environment, adsorption, separation, catalysis, and medicine.[2] One of the most common and effective routes to prepare such nanoporous carbons involves hard- and soft-templating methods, in which nanoporosity is generated by the removal of the hard or soft sacrificial component.[3] The most widely used hard templates, silica-based nanomaterials, are associated with a significant drawback, as removal of the sacrificial silica after carbonization requires harsh chemical treatments, such as an HF etch, which are generally hazardous, and may lead to loss of chemical functionality of heteroatom-enriched carbon.[3d,4] In contrast, organic sacrificial blocks used in soft templating are typically removed by thermal decomposition prior to carbonization without interfering with the chemistry of resultant carbon.[1a,5] As such, soft-templating methods are more facile and desirable. An example of such approach is the synthesis of carbons with ordered spherical or tubular mesostructures from carbon precursors (for example, resols) and self-assembling soft templates such as poly(ethylene oxide)–poly(propylene oxide)–poly(ethylene oxide) triblock copolymers.[2c,3e,5a,6] One of the difficulties associated with these methods is related to the fact that the noncovalent interactions between soft templates and carbon sources, such as hydrogen bonding, van der Waals forces, and electrostatic interaction, may be often too weak to robustly facilitate their self-assembly into well-defined mesostructures.[2c,7]

In the past, we have shown that this challenge can be addressed by integrating the heteroatom-rich polymeric carbon precursor, such as polyacrylonitrile (PAN), into the well-defined block copolymer templates synthesized using atom transfer radical polymerization (ATRP).[5b,d,8] We have also shown that with such copolymer-templated nitrogen-enriched porous carbons (CTNCs) of certain block copolymer compositions, it is possible to facilitate the formation of bicontinuous structures that resist collapse upon carbonization.[8] Carbons obtained from such precursors were shown to exhibit excellent performance as electrode materials for supercapacitors,[8a] as CO_2 sorbents[8b] or as electrocatalysts for oxygen reduction.[8a] One of the potential limitations of such copolymer-based templating is that the nanostructure of the precursor is strongly predicated on the well-known dependence on copolymer composition.[1d,9] We have demonstrated that this limitation can be overcome by using core–shell nanoparticle precursors synthesized by surface-initiated ATRP[10] (SI-ATRP) of PAN from the surface of sacrificial silica nanoparticles.[4c] One of the drawbacks of that system is that it still requires the aforementioned harsh chemical treatment to remove silica cores and generate nanoporosity.

Herein we describe a new remarkable method for templated synthesis of nanoporous carbons with well-defined spherical mesopores from all-organic nanostructured precursors prepared by ATRP. Precursors used in this method are comprised of hairy nanoparticles with organic sacrificial cores surrounded by covalently grafted nitrogen-rich carbon source

[*] Prof. Dr. D. Wu, Z. Li
Materials Science Institute, PCFM Lab and DSAPM Lab
School of Chemistry and Chemical Engineering
Sun Yat-sen University, Guangzhou 510275 (China)
E-mail: wudc@mail.sysu.edu.cn
Dr. M. J. Zhong, Prof. Dr. T. Kowalewski, Prof. Dr. K. Matyjaszewski
Department of Chemistry, Carnegie Mellon University
Pittsburgh, PA 15213 (USA)
E-mail: tomek@andrew.cmu.edu
km3b@andrew.cmu.edu

[**] This research was supported by the project of Guangdong Natural Science Funds for Distinguished Young Scholar (S2013050014408), NSFC (51173213, 51372280, 51172290, 51232005), Program for New Century Excellent Talents in University (NCET-12-0572), Program for Pearl River New Star of Science and Technology in Guangzhou (2013J2200015), Fundamental Research Funds for the Central Universities (13lgpy57), National Key Basic Research Program of China (2014CB932402), and the NSF (DMR-0969301).
ATRP = atom transfer radical polymerization.

Supporting information for this article is available on the WWW under http://dx.doi.org/10.1002/anie.201309836.

shell, for example *x*PMMA-*g*-PAN. Use of such shape-persistent building blocks assures that template nanostructures with continuous PAN precursor matrix can be formed robustly over a wide range of compositions. In contrast with current soft-templating and hard-templating methods, our new templating procedure eliminates any complicated self-assembly processes, works over a wide window of synthetic parameters, allows for a uniform filling of the template with heteroatom-enriched carbon source, and does not require the introduction of non-templated carbon sources, thus alleviating the formation of non-templated carbon by-products. Moreover, it should be pointed out that silica nanoparticles, typically used as a sacrificial component in hard templating processes, have to be removed using harsh treatments, such as HF etching, which could result in the destruction of critically important functionality afforded by the presence of heteroatoms. In contrast, the organic sacrificial cores used in our approach can be removed by simple thermal decomposition prior to carbonization without interference with the heteroatom afforded functionality of nanocarbon. Carbon materials prepared using this method exhibit well-defined templated mesoporosity, high surface area, and an abundance of nitrogen-containing functional groups.

The overall procedure for the preparation of nanoporous carbons is illustrated in Scheme 1. In the first step, *x*PMMA nanoparticles with Br initiating sites (*x*PMMA-Br) were synthesized using a microemulsion ATRP technique as reported before.[11] Subsequently, *x*PMMA-*g*-PAN hairy nanoparticles were fabricated by SI-ATRP from *x*PMMA-Br. In the final step, powders comprised of *x*PMMA-*g*-PAN hairy nanoparticles were subjected to oxidative stabilization[1d,8a] by heating in the presence of air to 280 °C and were carbonized under nitrogen at 500 or 800 °C. In this final step, the continuous PAN phase was transformed into nitrogen-enriched carbon framework, while the sacrificial *x*PMMA nanoparticles were thermally decomposed, generating uniformly distributed mesopores.

*x*PMMA-Br nanoparticles were synthesized using the microemulsion ATRP with ethyl 2-bromoisobutyrate (EBiB) initiator, methyl methacrylate (MMA) monomer, and ethylene glycol dimethacrylate (EGDMA) cross-linker under conditions specified in the Supporting Information, Table S1. As shown in Figure 1 A, dynamic light scattering (DLS) of nanoparticles formed after different polymerization times revealed that the hydrodynamic diameter (D_h) of nanoparticles increased from about 24 nm for $t = 0$ h to about 33 nm for $t = 1.5$ and 3 h. Such a modest size increase is indicative of the good stability of microemulsion ATRP. The reaction yield assessed by dividing the mass of purified

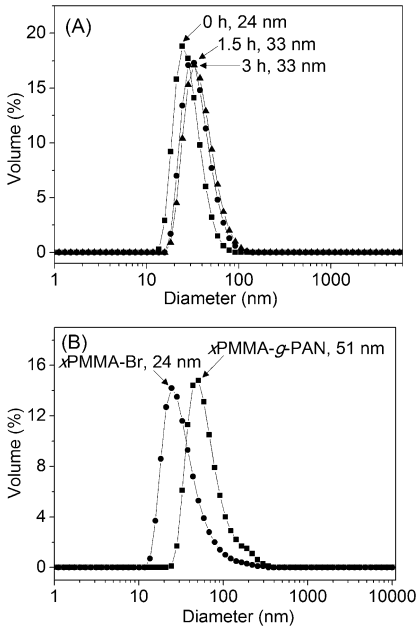

Figure 1. DLS hydrodynamic size distributions of A) the microemulsion latexes of *x*PMMA-Br at different polymerization times, and B) purified *x*PMMA-Br and *x*PMMA-*g*-PAN in DMF (1 mg mL^{-1}).

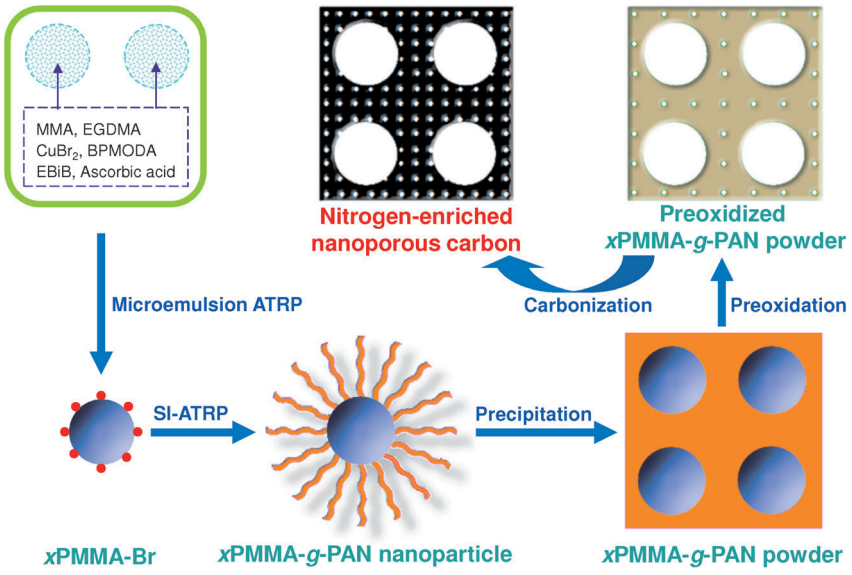

Scheme 1. Templated synthesis of nitrogen-enriched nanoporous carbons using all-organic hairy nanoparticles as building blocks.

*x*PMMA-Br product formed after 3 h by the initial total mass of MMA, EGDMA, and EBiB was equal to 36 wt %. The DLS diameter of the as-obtained *x*PMMA-Br in a 1 mg mL^{-1} dimethylformamide (DMF) dispersion was determined to be equal to 24 nm (Figure 1 B).

Such obtained *x*PMMA-Br nanoparticles were then used as a substrate for SI-ATRP grafting of acrylonitrile (AN) monomer (see conditions provided in the Supporting Information, Table S2). After quenching the polymerization, the suspension was deposited dropwise into methanol/water bath, filtered

and dried, yielding the *x*PMMA-*g*-PAN powder product. DLS of 1 mg mL^{-1} solution of such obtained *x*PMMA-*g*-PAN product in DMF (Figure 1B) revealed the presence of narrow and unimodal distribution of nanoparticles with the average hydrodynamic diameter approximately twice as high as one observed for *x*PMMA-Br nanoparticles (51 versus 24 nm). The grafting-induced size increase is also confirmed by comparison of TEM images (Supporting Information, Figure S1A and S1B). Such prominent increase of the particle size was the clear indication of successful grafting of PAN from *x*PMMA-Br. Accordingly, the gravimetric ratio of PAN to *x*PMMA estimated from the mass increase upon grafting was equal to 3:2 or circa 60 wt %. Similar result was obtained from the elemental analysis which showed that the mass percentage of N in the *x*PMMA-*g*-PAN powder was equal to 16.5 wt %, corresponding to 62.5 wt % of PAN. Following the precipitation step, the hairy *x*PMMA-*g*-PAN nanoparticles consolidated into a bulk solid in which the *x*PMMA cores could not be differentiated from the continuous PAN matrix owing to limited electron density contrast between two phases (see the TEM image shown in Figure S1C).

*x*PMMA-*g*-PAN powders were converted into nitrogen-enriched nanoporous carbons (NNCs) by preoxidation at 280 °C for 6 h in an air flow followed by carbonization through heating under N_2 to 500 or 800 °C at a heating rate of 5 °C min^{-1}. During the preoxidation treatment, the PAN chains were chemically stabilized by oxidative intra-/inter-chain cross-linking and side-group cyclization.[1d,12] As shown in our previous work, such chemical stabilization assures preservation of PAN nanostructure upon carbonization.[4b,8] Concomitantly with the preoxidation and carbonization treatment, the sacrificial *x*PMMA nanoparticle cores were thermally decomposed, leading to the formation of uniformly distributed spherical mesopores evident in the TEM image shown in Figure 2. The generation and evolution of porosity in the process of preoxidation and carbonization was quantitatively characterized by N_2 adsorption at 77 K (Figure S2). The evolution of pore size distributions upon thermal stabilization and carbonization of *x*PMMA-*g*-PAN determined by the density functional theory (DFT) approach is shown in Figure 3. Clearly, mesopores with diameter of 8.6 nm (Figure 3) formed already during the oxidative annealing treatment indicating that the sacrificial *x*PMMA cores already underwent thermal decomposition at this step,

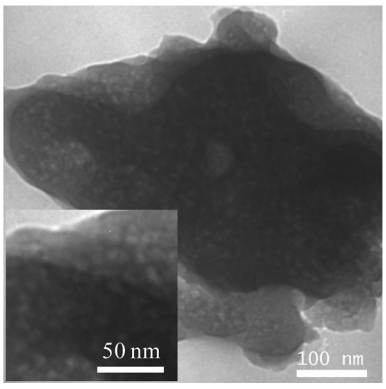

Figure 2. TEM image of NNC-800.

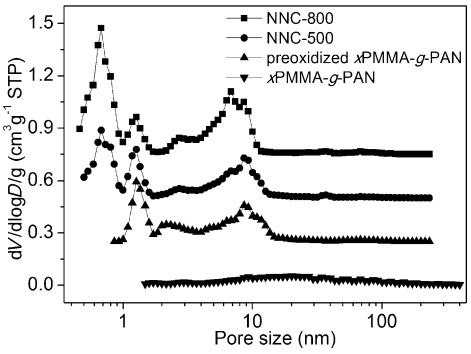

Figure 3. DFT pore size distributions of *x*PMMA-*g*-PAN powder, preoxidized *x*PMMA-*g*-PAN powder, NNC-500, and NNC-800. The curves of the latter three are offset vertically by 0.25, 0.50, and 0.75 cm^3 g^{-1} STP, respectively.

as also indicated by concomitant 92 % weight loss observed in a control experiment where *x*PMMA-Br was treated at 280 °C for 6 h in an air flow. Interestingly, as shown in Figure 3, oxidative annealing led also to the formation of 1.3 nm pores in the PAN framework, which is presumably due to its non-uniform shrinkage upon cross-linking or burn-off of non-carbon elements and carbon-containing compounds. Upon further increase of temperature to 500–800 °C additional micropores of smaller diameter (0.7 nm) were generated, and the size of mesopores decreased slightly to 6.8 nm at 800 °C, which can be attributed to the shrinkage of the framework upon carbonization. Accordingly, the Brunauer–Emmett–Teller (BET) specific surface area (S_{BET}) increased to 487 m^2 g^{-1} with the increase of carbonization temperature (Figure S3), which can be ascribed to the formation of mesopores and additional micropores during oxidative annealing and carbonization (Figure S4). Furthermore, combustion elemental analysis revealed that NNC-500 and NNC-800 possessed, respectively, high degree nitrogen contents of 20.7 and 10.2 wt %, originating from the nitrogen-rich PAN precursor (Table S3).

Owing to their well-defined porosity and high nitrogen content, NNCs developed in this study, just like their previously demonstrated CTNC counterparts,[8] hold considerable promise in a wide range of applications. For example, NNC-500 and NNC-800 exhibited, respectively, CO_2 adsorption capacities of 2.4 and 3.2 mmol g^{-1} at 0 °C (Figure S5A), which are comparable with those for other nanocarbons, such as CTNC-800,[8b] CMK-3,[13] and HCM-DAH-1.[5c] Another example is the use of NNCs as supercapacitor electrodes. NNC-800 exhibited a high specific capacitance of 261 F g^{-1} at a current density of 20 mA g^{-1} (Figure S5B), a value similar to those for other nanocarbons.[1e,14] Notably, the performance of NNCs is comparable to that of nanocarbons prepared by traditional means and has been achieved without any optimization of their synthesis. Further major performance improvements can be envisioned given inherently broad tunability of materials prepared according to our method (for example, by variation of composition, thermal stabilization conditions, pyrolysis conditions, and so on).

In conclusion, we have demonstrated a versatile ATRP-based templating method for preparation of nitrogen-

enriched nanoporous carbon materials using hairy *x*PMMA-*g*-PAN nanoparticles as building blocks. Owing to the presence of a strong covalent interaction between the templates and carbon sources, *x*PMMA cores were uniformly distributed in the continuous PAN phase during precipitation of *x*PMMA-*g*-PAN nanoparticles to produce *x*PMMA-*g*-PAN powder. As such, the well-distributed *x*PMMA cores can act as the template for generating mesopores, because of their thermal decomposability during preoxidation of *x*PMMA-*g*-PAN powder. Moreover, increasing the pyrolysis temperature facilitated the generation of more micropores. Meanwhile, high contents of nitrogen groups were achieved in the PAN-derived carbon framework. Thus, such prepared NNCs demonstrated well-developed hierarchical porosity, large surface area, and high-level nitrogen doping. We anticipate that the templating concept based on shape-persistent all-organic nanostructured precursors prepared by ATRP presented herein will lead to advancement of understanding of fundamentals of fabrication of functional carbon materials with a broad range of applications in the fields such as energy, adsorption, separation, catalysis, and medicine.

Received: November 12, 2013
Published online: March 5, 2014

Keywords: CO_2 capture · functional nanocarbons · supercapacitors · ATRP

[1] a) C. Liang, Z. Li, S. Dai, *Angew. Chem.* **2008**, *120*, 3754 – 3776; *Angew. Chem. Int. Ed.* **2008**, *47*, 3696 – 3717; b) D. Wu, F. Xu, B. Sun, R. Fu, H. He, K. Matyjaszewski, *Chem. Rev.* **2012**, *112*, 3959 – 4015; c) D. S. Su, R. Schlögl, *ChemSusChem* **2010**, *3*, 136 – 168; d) J. P. McGann, M. J. Zhong, E. K. Kim, S. Natesakhawat, M. Jaroniec, J. F. Whitacre, K. Matyjaszewski, T. Kowalewski, *Macromol. Chem. Phys.* **2012**, *213*, 1078 – 1090; e) H. L. Jiang, B. Liu, Y. Q. Lan, K. Kuratani, T. Akita, H. Shioyama, F. Zong, Q. Xu, *J. Am. Chem. Soc.* **2011**, *133*, 11854 – 11857; f) M. Hu, J. Reboul, S. Furukawa, N. L. Torad, Q. Ji, P. Srinivasu, K. Ariga, S. Kitagawa, Y. Yamauchi, *J. Am. Chem. Soc.* **2012**, *134*, 2864 – 2867; g) Q. Xiang, J. Yu, M. Jaroniec, *J. Am. Chem. Soc.* **2012**, *134*, 6575 – 6578; h) M. Antonietti, N. Fechler, T. P. Fellinger, *Chem. Mater.* **2014**, *26*, 196 – 210; i) N. Fechler, T. P. Fellinger, M. Antonietti, *Adv. Mater.* **2013**, *25*, 75 – 79.

[2] a) D. S. Su, S. Perathoner, G. Centi, *Chem. Rev.* **2013**, *113*, 5782 – 5816; b) S. Yang, X. Feng, L. Zhi, Q. Cao, J. Maier, K. Müllen, *Adv. Mater.* **2010**, *22*, 838 – 842; c) Y. R. Liang, R. W. Fu, D. C. Wu, *Acs Nano* **2013**, *7*, 1748 – 1754; d) D. W. Wang, F. Li, M. Liu, G. Q. Lu, H. M. Cheng, *Angew. Chem.* **2008**, *120*, 379 – 382; *Angew. Chem. Int. Ed.* **2008**, *47*, 373 – 376; e) S. Li, Y. Luo, W. Lv, W. Yu, S. Wu, P. Hou, Q. Yang, Q. Meng, C. Liu, H.-M. Cheng, *Adv. Energy Mater.* **2011**, *1*, 486 – 490; f) S. Song, Y. Liang, Z. Li, Y. Wang, R. Fu, D. Wu, P. Tsiakaras, *Appl. Catal. B* **2010**, *98*, 132 – 137; g) Y. Fang, B. Luo, Y. Jia, X. Li, B. Wang, Q. Song, F. Kang, L. Zhi, *Adv. Mater.* **2012**, *24*, 6348 – 6355; h) V. Presser, J. McDonough, S.-H. Yeon, Y. Gogotsi, *Energy Environ. Sci.* **2011**, *4*, 3059 – 3066; i) S. B. Yang, R. E. Bachman, X. L. Feng, K. Müllen, *Acc. Chem. Res.* **2013**, *46*, 116 – 128; j) X. Li, M. Antonietti, *Chem. Soc. Rev.* **2013**, *42*, 6593 – 6604; k) T. P. Fellinger, F. Hasché, P. Strasser, M. Antonietti, *J. Am. Chem. Soc.* **2012**, *134*, 4072 – 4075.

[3] a) H. Nishihara, Q. H. Yang, P. X. Hou, M. Unno, S. Yamauchi, R. Saito, J. I. Paredes, A. Martinez-Alonso, J. M. D. Tascon, Y. Sato, M. Terauchi, T. Kyotani, *Carbon* **2009**, *47*, 1220 – 1230; b) D. C. Wu, C. M. Hui, H. C. Dong, J. Pietrasik, H. J. Ryu, Z. H. Li, M. J. Zhong, H. K. He, E. K. Kim, M. Jaroniec, T. Kowalewski, K. Matyjaszewski, *Macromolecules* **2011**, *44*, 5846 – 5849; c) R. Liu, S. M. Mahurin, C. Li, R. R. Unocic, J. C. Idrobo, H. Gao, S. J. Pennycook, S. Dai, *Angew. Chem.* **2011**, *123*, 6931 – 6934; *Angew. Chem. Int. Ed.* **2011**, *50*, 6799 – 6802; d) A. H. Lu, F. Schüth, *Adv. Mater.* **2006**, *18*, 1793 – 1805; e) Y. Fang, Y. Y. Lv, R. C. Che, H. Y. Wu, X. H. Zhang, D. Gu, G. F. Zheng, D. Y. Zhao, *J. Am. Chem. Soc.* **2013**, *135*, 1524 – 1530; f) T. Kowalewski, N. V. Tsarevsky, K. Matyjaszewski, *J. Am. Chem. Soc.* **2002**, *124*, 10632 – 10633.

[4] a) B. H. Han, W. Zhou, A. Sayari, *J. Am. Chem. Soc.* **2003**, *125*, 3444 – 3445; b) D. Wu, H. Dong, J. Pietrasik, E. K. Kim, C. M. Hui, M. Zhong, M. Jaroniec, T. Kowalewski, K. Matyjaszewski, *Chem. Mater.* **2011**, *23*, 2024 – 2026; c) C. Tang, L. Bombalski, M. Kruk, M. Jaroniec, K. Matyjaszewski, T. Kowalewski, *Adv. Mater.* **2008**, *20*, 1516 – 1522.

[5] a) Y. Wan, Y. F. Shi, D. Y. Zhao, *Chem. Mater.* **2008**, *20*, 932 – 945; b) C. B. Tang, A. Tracz, M. Kruk, R. Zhang, D. M. Smilgies, K. Matyjaszewski, T. Kowalewski, *J. Am. Chem. Soc.* **2005**, *127*, 6918 – 6919; c) G. P. Hao, W. C. Li, D. Qian, G. H. Wang, W. P. Zhang, T. Zhang, A. Q. Wang, F. Schuth, H. J. Bongard, A. H. Lu, *J. Am. Chem. Soc.* **2011**, *133*, 11378 – 11388; d) M. J. Zhong, C. B. Tang, E. K. Kim, M. Kruk, E. B. Celer, M. Jaroniec, K. Matyjaszewski, T. Kowalewski, *Mater. Horiz.* **2014**, *1*, 121 – 124.

[6] Y. Fang, D. Gu, Y. Zou, Z. Wu, F. Li, R. Che, Y. Deng, B. Tu, D. Zhao, *Angew. Chem.* **2010**, *122*, 8159 – 8163; *Angew. Chem. Int. Ed.* **2010**, *49*, 7987 – 7991.

[7] Y. R. Liang, S. H. Lu, D. C. Wu, B. Sun, F. Xu, R. W. Fu, *J. Mater. Chem. A* **2013**, *1*, 3061 – 3067.

[8] a) M. Zhong, E. K. Kim, J. P. McGann, S. E. Chun, J. F. Whitacre, M. Jaroniec, K. Matyjaszewski, T. Kowalewski, *J. Am. Chem. Soc.* **2012**, *134*, 14846 – 14857; b) M. J. Zhong, S. Natesakhawat, J. P. Baltrus, D. Luebke, H. Nulwala, K. Matyjaszewski, T. Kowalewski, *Chem. Commun.* **2012**, *48*, 11516 – 11518.

[9] K. Matyjaszewski, *Prog. Polym. Sci.* **2005**, *30*, 858 – 875.

[10] a) J. Pyun, S. J. Jia, T. Kowalewski, G. D. Patterson, K. Matyjaszewski, *Macromolecules* **2003**, *36*, 5094 – 5104; b) L. Bombalski, H. C. Dong, J. Listak, K. Matyjaszewski, M. R. Bockstaller, *Adv. Mater.* **2007**, *19*, 4486 – 4490; c) J. Choi, H. Dong, K. Matyjaszewski, M. R. Bockstaller, *J. Am. Chem. Soc.* **2010**, *132*, 12537 – 12539; d) K. Matyjaszewski, N. V. Tsarevsky, *Nat. Chem.* **2009**, *1*, 276 – 288; e) K. Matyjaszewski, J. Xia, *Chem. Rev.* **2001**, *101*, 2921 – 2990.

[11] a) K. Min, H. F. Gao, J. A. Yoon, W. Wu, T. Kowalewski, K. Matyjaszewski, *Macromolecules* **2009**, *42*, 1597 – 1603; b) K. Min, H. F. Gao, K. Matyjaszewski, *J. Am. Chem. Soc.* **2005**, *127*, 3825 – 3830.

[12] P. Bajaj, A. K. Roopanwal, *J. Macromol. Sci. Rev. Macromol. Chem. Phys.* **1997**, *37*, 97 – 147.

[13] M. Sevilla, A. B. Fuertes, *J. Colloid Interface Sci.* **2012**, *366*, 147 – 154.

[14] a) Z. Wen, X. Wang, S. Mao, Z. Bo, H. Kim, S. Cui, G. Lu, X. Feng, J. Chen, *Adv. Mater.* **2012**, *24*, 5610 – 5616; b) X. Feng, Y. Liang, L. Zhi, A. Thomas, D. Wu, I. Lieberwirth, U. Kolb, K. Müllen, *Adv. Funct. Mater.* **2009**, *19*, 2125 – 2129; c) Z. Fan, J. Yan, L. Zhi, Q. Zhang, T. Wei, J. Feng, M. Zhang, W. Qian, F. Wei, *Adv. Mater.* **2010**, *22*, 3723 – 3728; d) K. H. An, W. S. Kim, Y. S. Park, J. M. Moon, D. J. Bae, S. C. Lim, Y. S. Lee, Y. H. Lee, *Adv. Funct. Mater.* **2001**, *11*, 387 – 392; e) N. P. Wickramaratne, V. S. Perera, B.-W. Park, M. Gao, G. W. McGimpsey, S. D. Huang, M. Jaroniec, *Chem. Mater.* **2013**, *25*, 2803 – 2811.

